Wave function statistics for ballistic quantum transport through chaotic open billiards: Statistical crossover and coexistence of regular and chaotic waves

Hiromu Ishio,[1,2] Alexander I. Saichev,[1,3] Almas F. Sadreev,[1,4] and Karl-Fredrik Berggren[1]
[1]*Department of Physics and Measurement Technology, Linköping University, S-581 83 Linköping, Sweden*
[2]*School of Mathematics, University of Bristol, University Walk, Bristol BS8 1TW, England*
[3]*Department of Radiophysics, Nizhny Novgorod State University, Gagarin prospekt 23, 603600, Nizhny Novgorod, Russia*
[4]*Kirensky Institute of Physics, 660036, Krasnoyarsk, Russia*
(Received 26 February 2001; published 18 October 2001)

For ballistic transport through chaotic open billiards, we implement accurate fully quantal calculations of the probability distributions and spatial correlations of the local densities of single-electron wave functions within the cavity. We find wave-statistical behaviors intrinsically different from those in their closed counterparts. Chaotic-scattering wave functions in open systems can be quantitatively interpreted in terms of statistically independent real and imaginary random fields in the same way as for wave-function statistics of closed systems in the time-reversal symmetry-breaking crossover regime. We also discuss perceived statistical deviations, which are attributed to the coexistence of regular and chaotic waves and given analytical explanations.

DOI: 10.1103/PhysRevE.64.056208 PACS number(s): 05.60.Gg, 05.45.Mt, 73.23.Ad

I. INTRODUCTION

Complexity in the quantum mechanical behavior of classically nonintegrable systems may be one of the most intriguing subjects in the field of quantum chaos. The study of morphological complexity in the eigenstates of chaotic billiards has been actively carried out [1]. The properties of nodal lines (or points) in the wave dynamics are closely related to spectral geometry in optics [2].

Historically, McDonald and Kaufman first numerically revealed the complicated eigen function structures in a closed two dimensional (2D) chaotic billiard [3]. We denote the scaled local density as $y(\mathbf{r})=V|\psi(\mathbf{r})|^2$, where V is the volume of the system, in which a single-particle wave function $\psi(\mathbf{r})$ is normalized in terms of the position $\mathbf{r}$. It is well known that the probability distribution of the local densities of a chaotic eigenfunction of a closed system is the Porter-Thomas (PT) distribution [4],

$$P(y)=(1/\sqrt{2\pi y})\exp(-y/2), \tag{1.1}$$

described by a Gaussian orthogonal ensemble (GOE) of random matrices, when time-reversal symmetry (TRS) is present, i.e., $\psi\in\mathbb{R}$. On the other hand, the distribution is an exponential [4,5],

$$P(y)=\exp(-y), \tag{1.2}$$

described by a Gaussian unitary ensemble (GUE) of random matrices, when TRS is broken in the closed system, i.e., $\psi\in\mathbb{C}$. ψ has nodal lines in the former case while it has nodal points in the latter case. At the same time, Berry has discussed the coordinate dependence of the semiclassical wave function in the classically chaotic regime, adopting an idea of an infinite superposition of plane waves with a fixed wave number k, but with random directions and amplitudes (so-called Berry function) [6]. He showed that the space-averaged spatial correlation of the 2D wave function is given by

$$\langle\psi(\mathbf{r}_1)\psi^*(\mathbf{r}_2)\rangle=\text{const}\times J_0(kr), \tag{1.3}$$

where $r\equiv|\mathbf{r}_1-\mathbf{r}_2|$ and $J_0(x)$ is the Bessel function of zeroth order. Later, within the super-symmetry formalism, the disorder-averaged (equivalently space-averaged) spatial correlation of the local densities in disordered (i.e., chaotic) 2D billiards was found to be [5,7]

$$P_2(kr)\equiv\langle y(\mathbf{r}_1)y(\mathbf{r}_2)\rangle=1+cJ_0^2(kr), \tag{1.4}$$

where $c=2$ for GOE (TRS) and $c=1$ for GUE (broken TRS) eigenfunctions.

Investigations of the continuous transition of the wave-function statistics between GOE and GUE symmetries have been also worked out. Assuming a complex wave function, $\psi=u+w$, where u and v are independent random variables with a common mean value $\langle u\rangle=\langle v\rangle=0$, a common variance $\langle u^2\rangle=\langle v^2\rangle=1$ and $\langle uv\rangle=0$, we introduce a transition parameter $b\in(1,2]$ into the weights for u and v as $\psi=\sqrt{1/b}u+i\sqrt{1-1/b}v$. Then we have the probability distribution [8–12]:

$$P(y)=\frac{b}{2\sqrt{b-1}}\exp\left(-\frac{b^2}{4(b-1)}y\right)I_0\left(\frac{b(2-b)}{4(b-1)}y\right), \tag{1.5}$$

where $I_0(x)$ is the modified Bessel function of zeroth order, and the spatial correlation [13]:

$$P_2(kr)=1+\left[1+\left(\frac{2-b}{b}\right)^2\right]J_0^2(kr). \tag{1.6}$$

For $b\to1$ and $b\to2$, both equations tend to the GOE and GUE cases, respectively. We should note that the transition (1.5) may be described as well by other probability distribution functions derived by an interpolation of the χ_ν^2 distribution with ν continuously varying between 1 and 2 [14], an energy averaging of the random matrix elements of Hamiltonians representing the GOE-GUE crossover [15] and the

 ©2001 The American Physical Society

supersymmetry method for disordered (imperfectly open) systems in an arbitrary magnetic field [16]. However, the assumption of independent fluctuations for u and v in the derivation of Eqs. (1.5) and (1.6) is most naturally adopted in the context of this paper, as we will see later. Experimental agreement with these theoretical predictions is obtained using thin microwave cavities with TRS [17,18], without TRS [18], and in the TRS-breaking crossover regime [13]. The predictions are also confirmed numerically for closed billiards with TRS [19–23]. On the other hand, there is also a remarkable work for a ''partially'' open chaotic resonator [24]: Assuming a real random matrix model associated with the internal real eigenfunctions with a *PT* distribution and adding an imaginary effective potential representing a probing point contact, the authors showed that the density distribution of the wave function at the point contact coincides with Eq. (1.5).

All the conventional considerations mentioned above, however, are basically concerned with closed systems or in the limit of *imperfect* coupling. To the best of our knowledge, one work was carried out for the wave-density distribution and its joint probability distribution in relation to *perfect* coupling to the environment [11]. Using independent Gaussian variables for $\mathrm{Re}\,\psi$ and $\mathrm{Im}\,\psi$ following from the central limit theorem to great number of random wave superpositions, they derived Eq. (1.5) for the wave-density distribution in the crossover regime between closed and open systems. Nevertheless, the way how to identify the independent random variables in general situations, the validity of the random variable assumption in real systems etc. still remain unclarified in spite of the fact that they are more closely related to experimental situations.

The aim of this paper is to give deeper insight into the wave statistics for perfectly open systems by considering ballistic quantum transport through chaotic open billiards with no magnetic field. In Sec. II, we explicitly discuss time reversibility, space reciprocity breaking and resulting wave statistical crossover in the open systems. We present an alternative simple derivation of Eqs. (1.5) and (1.6) in Sec. III. More importantly, we also show how to identify the two independent random fields in a given wave function. We will find in Sec. IV that Eqs. (1.5) and (1.6) for the crossover regime are applicable to the ballistic transport through chaotic open billiards. We also discuss statistical deviations attributed to the coexistence of regular and chaotic waves. Section V consists of conclusions.

II. TIME REVERSIBILITY, SPACE RECIPROCITY BREAKING AND WAVE STATISTICAL CROSSOVER

It is essential that the scattering wave function, ψ_s, in the open systems is no more a real function in general, i.e., it is different from an eigenfunction of time-reversal closed systems. It is because the *space reciprocity* in conservative closed systems, which means that each plane wave in the Berry function ties up with its counterpart with the same amplitude and running in the opposite direction in phase, is lost by coupling to the environment in open systems. This requires the use of boundary conditions allowing for the nonzero probability current density: $\mathbf{j}(\mathbf{r}) = (\hbar/m)\mathrm{Im}[\psi_s^*(\mathbf{r})\nabla\psi_s(\mathbf{r})]$. Such boundary conditions can be naturally obtained only for complex wave functions prescribing the distribution of incoming flows on the boundary. On the other hand, the Hamiltonian operator, $\hat{\mathcal{H}}$, of the system in our case is real and invariant on reverse of time $\hat{\mathcal{T}}$: $t \to -t$ by definition. Therefore, the real and imaginary parts of scattering state, $\psi_s(=u_s+iv_s)$, are independent solutions of the time-independent Schrödinger equation for a stationary state. In other words, for an incoming wave $\psi_0=u_0+iv_0$, u_s and v_s can respond in different manners inside the scattering domain, which are determined by the initial wave components, u_0 and v_0 [e.g., Neumann and Dirichlet boundary conditions, respectively, for a plane wave $\psi_0 \sim \cos(\mathbf{k}\cdot\mathbf{r}) + i\sin(\mathbf{k}\cdot\mathbf{r})$ at a boundary $\mathbf{k}\cdot\mathbf{r}=0$]. This fact is remarkable when we apply the random matrix theory (RMT) to the wave-function statistics in open systems. It is expected that (i) the resulting statistics is close to the GOE if u_s and v_s are strongly correlated (i.e., ψ_s can be expressed with real functions only), while (ii) it is the GUE if they are completely uncorrelated (i.e., u_s and v_s are statistically independent and have equal weight). An extreme example of the case (i) is a single-mode total reflection where the entire space reciprocity recovers and the GOE statistics holds completely. The weak localization effect, i.e., coherent backscattering by time-reversed paths, partially plays the same role, however, it may be hard to distinguish this effect from another if both coexist. In any case, the value of b may provide a quantitative measure of the degree of the space-reciprocity breaking in open systems.

Finally, we should remark that the expressions for the scattering wave statistics in open systems are in complete analogy with those for the eigenfunction statistics in closed systems with broken TRS [11]. This is because boundary conditions allowing for $\mathbf{j}(\neq 0)$ are introduced for a solution of the dynamical state with broken TRS in the case of open systems, and not because coupling to the environment breaks the TRS of the dynamics itself, which is completely determined by $\hat{\mathcal{H}}$.

III. ANALYTICAL SIMPLE DERIVATION OF WAVE-FUNCTION STATISTICS IN THE CROSSOVER REGIME

We start with a simple but essential assumption that an arbitrary chaotic-scattering wave function, $\psi_s(\mathbf{r})$, for a single particle is related to its *canonical form* by

$$\psi_s(\mathbf{r}) = e^{i\alpha}\psi(\mathbf{r}), \tag{3.1}$$

where $\psi(\mathbf{r})$ is a phase-invariant canonical wave function whose real and imaginary parts can be viewed as statistically independent Gaussian random fields. The rotation phase factor, α, is attributed to the correlation between the two Gaussian random fields. It is dependent on each system and can be identified in experimental measurements or numerical simulations.

We first derive the canonical form of $\psi_s(\mathbf{r})=u_s(\mathbf{r})+iv_s(\mathbf{r})$. In sufficient large systems compared to the wave length, u_s and v_s can be regarded as random and $\langle u_s\rangle$

$=\langle v_s\rangle=0$. We introduce next notations: $\sigma_u^2=\langle u_s^2\rangle$, $\sigma_v^2=\langle v_s^2\rangle$, $\sigma_{uv}=\langle u_s v_s\rangle$, and $\sigma^2=\sigma_u^2+\sigma_v^2=\langle|\psi_s|^2\rangle$. We multiply both sides of Eq. (3.1) by $e^{-i\alpha}$:

$$\psi=e^{-i\alpha}\psi_s\equiv p+iq. \tag{3.2}$$

Here p and q are real and imaginary parts of ψ, respectively, and

$$p=u_s\cos\alpha+v_s\sin\alpha, \quad q=-u_s\sin\alpha+v_s\cos\alpha. \tag{3.3}$$

We have to choose α in such a way that p and q become statistically independent: $\langle pq\rangle=0$. Therefore, we get

$$\tan 2\alpha=\frac{2\sigma_{uv}}{\sigma_u^2-\sigma_v^2}. \tag{3.4}$$

It is easy to show that the variances of p and q are equal to

$$\langle p^2\rangle=\frac{1}{2}[\sigma^2+\sqrt{\sigma^4-4(\sigma_u^2\sigma_v^2-\sigma_{uv}^2)}],$$

$$\langle q^2\rangle=\frac{1}{2}[\sigma^2-\sqrt{\sigma-4(\sigma_u^2\sigma_v^2-\sigma_{uv}^2)}]. \tag{3.5}$$

Here we assumed $\sigma_u^2\geqslant\sigma_v^2$ without losing generality, because we can always multiply ψ_s by $\pm i$ (or equivalently $\alpha\rightarrow\alpha\pm\pi/2$), if necessary, and then choose $\alpha\in[-\pi/4,\pi/4]$ from Eq. (3.4). We note that both $\langle p^2\rangle$ and $\langle q^2\rangle$ are independent of α. Introducing a parameter $\varepsilon(0\leqslant\varepsilon\leqslant 1)$ as $\langle q^2\rangle/\langle p^2\rangle\equiv\varepsilon^2$, and together with the relation $\langle p^2\rangle+\langle q^2\rangle=\sigma^2$, we obtain $\langle p^2\rangle=[1/(1+\varepsilon^2)]\sigma^2$ and $\langle q^2\rangle=[\varepsilon^2/(1+\varepsilon^2)]\sigma^2$. Then we reach the canonical form:

$$\psi(\mathbf{r})=\left[\frac{u(\mathbf{r})+i\varepsilon v(\mathbf{r})}{\sqrt{1+\varepsilon^2}}\right]\sigma, \tag{3.6}$$

where $u(\mathbf{r})$ and $v(\mathbf{r})$ are statistically independent Gaussian random fields with $\langle u\rangle=\langle v\rangle=\langle uv\rangle=0$, $\langle u^2\rangle=\langle v^2\rangle=1$ and a Bessel correlation function (1.3). The parameter ε is calculated by

$$\varepsilon=\sqrt{\frac{1-\delta}{1+\delta}}, \tag{3.7}$$

where

$$\delta\equiv\frac{\langle p^2\rangle-\langle q^2\rangle}{\sigma^2}=\frac{1}{\sigma^2}\sqrt{\sigma^4-4(\sigma_u^2\sigma_v^2-\sigma_{uv}^2)}. \tag{3.8}$$

The value of ε shows the degree of correlation between u_s and v_s. We have $\varepsilon=0$ in the case that u_s and v_s are completely correlated as in the case of time-reversal closed systems while we have $\varepsilon=1$ if u_s and v_s are completely uncorrelated, i.e., the Berry function. In the following discussion, σ^2 [and σ in Eq. (3.6)] is chosen to be unity, corresponding to the normalization, $\langle|\psi_s|^2\rangle(=\langle|\psi|^2\rangle)\equiv 1$.

In particular, the random wave density in the system is equal to

$$\rho_\varepsilon(\mathbf{r})=\frac{u^2(\mathbf{r})+\varepsilon^2 v^2(\mathbf{r})}{1+\varepsilon^2}. \tag{3.9}$$

In the following, we investigate statistical dependence of the normalized random wave density (3.9) on the parameter ε. [An analogous derivation of Eq. (3.15) is found in Ref. [11]. In their theory, however, the value of ε is not determined for a given wave in general situations.]

We recall that chaotic wave densities in closed systems follow the PT distribution (1.1) whose singularity at $\rho=0$ is stipulated by the characteristic behavior of $u^2(\mathbf{r})$ in the vicinity of ''self-avoiding'' nodal lines. In open systems, nodal lines are disappeared for any $\varepsilon>0$, and, as a result, the singularity of the density distribution (1.1) is eliminated. This becomes evident when we calculate the distribution of the random wave density (3.9) for arbitrary ε.

We consider the cumulative distribution of the wave densities. It is equal to the probability

$$G_\varepsilon(\rho)=P\left(\frac{u^2+w^2}{1+\varepsilon^2}<\rho\right), \tag{3.10}$$

where we used the auxiliary random field $w(\mathbf{r})=\varepsilon v(\mathbf{r})$. The probability (3.10) is equal to

$$G_\varepsilon(\rho)=\int\int_{C(\rho,\varepsilon)} f(u,w)\,du\,dw, \tag{3.11}$$

where $C(\rho,\varepsilon)$ is a circle in the plane $\{u, w\}$, centered at the origin and with radius $\sqrt{(1+\varepsilon^2)\rho}$. Now, we take into account that $f(u,w)$ is a joint distribution of Gaussian random values u, w and has the form

$$f(u,w)=\frac{1}{2\pi\varepsilon}\exp\left[-\frac{1}{2}\left(u^2+\frac{1}{\varepsilon^2}w^2\right)\right]. \tag{3.12}$$

Substituting this distribution into the integral (3.11), we get

$$G_\varepsilon(\rho)=\frac{1}{2\pi}\int_0^{2\pi}\frac{1-\exp[-\rho\mu(\mu+\nu\cos\theta)]}{\mu+\nu\cos\theta}\,d\theta. \tag{3.13}$$

Here we used the notations:

$$\mu=\frac{1}{2}\left(\frac{1}{\varepsilon}+\varepsilon\right), \quad \nu=\frac{1}{2}\left(\frac{1}{\varepsilon}-\varepsilon\right) \quad (\mu+\nu=1/\varepsilon, \quad \mu-\nu=\varepsilon). \tag{3.14}$$

After differentiating both sides of Eq. (3.13) with respect to ρ, we get the wave-density distribution,

$$f_\varepsilon(\rho)=\mu\exp(-\mu^2\rho)I_0(\mu\nu\rho), \tag{3.15}$$

where $I_0(x)$ is the modified Bessel function of zeroth order.

Next, we derive wave-density correlation function depending on ε. Using the rule of fourth moments of Gaussian random fields splitting [5,7], it is easy to show that the correlation function is equal to

$$b_\rho(s)=\langle \rho_\varepsilon(\mathbf{r})\rho_\varepsilon(\mathbf{r}+\mathbf{s})\rangle$$
$$=\frac{\langle [u^2(\mathbf{r})+\varepsilon^2 v^2(\mathbf{r})][u^2(\mathbf{r}+\mathbf{s})+\varepsilon^2 v^2(\mathbf{r}+\mathbf{s})]\rangle}{(1+\varepsilon^2)^2}$$
$$=1+c(\varepsilon)J_0^2(ks), \tag{3.16}$$

where the coefficient

$$c(\varepsilon)=2\frac{1+\varepsilon^4}{(1+\varepsilon^2)^2} \tag{3.17}$$

describes the influence of openness on the wave-density correlation function.

Finally, we notice that, by defining

$$\varepsilon\equiv\sqrt{b-1}, \tag{3.18}$$

Eqs. (3.15) and (3.16) coincide with Eqs. (1.5) and (1.6) obtained by RMT, respectively.

IV. NUMERICAL ANALYSES AND DISCUSSIONS

For numerical analyses, we consider a 2D Bunimovich stadium billiard [25]. It is characterized by the radius of a semicircle a and the half-length of a straight section l. The maximum Lyapunov exponent reaches its maximum at the fully chaotic limit ($a=l$) [26]. In the following, we simply refer to this limit as the stadium. The billiard is coupled to a pair of leads with a common width d.

In quantum dynamics, the dc current passes through the leads. We solve the time-independent Schrödinger equation for a single electron under Dirichlet boundary conditions based on the plane-wave-expansion method [27], giving reflection and transmission amplitudes as well as local wave functions for each energy.

Figure 1 shows transmission probability T as a function of Fermi wave number k for the incoming wave with propagating mode n in the lead. T is directly connected to conductance of the system [28]. We see a sequence of overlapping resonances that are broader in the high-energy region [Fig. 1(b)] than they are in the low-energy region [Fig. 1(a)]. As typical situations for statistical investigations of the scattering wave functions, we consider five points marked with $A \sim E$ in Fig. 1: $T\simeq 0$ (A), 0.5 (B), 1 (C) for $n=1$ in the low-energy region and $T\neq 0$, 1 for $n=1$ (D), 4 (E) in the high-energy region. In the calculation of the statistics, the spatial average is taken in the cavity region corresponding to the closed stadium. For convenience, the area, $\mathcal{A}(=V)$, of the cavity region is normalized to be unity.

Figure 2 shows the results of the numerical calculations of the probability distribution $P(|\psi|^2)$ and spatial correlation $P_2(kr)$ together with their analytical predictions in which the parameter b was determined numerically by Eqs. (3.7) and (3.18). Correspondingly, Fig. 3 shows the wave probability, density, and nodal lines.

In Fig. 2(a), we see that both $P(|\psi|^2)$ and $P_2(kr)$ are very close to the GOE predictions due to the almost total reflection of the initial wave. We recognize the space reciprocity

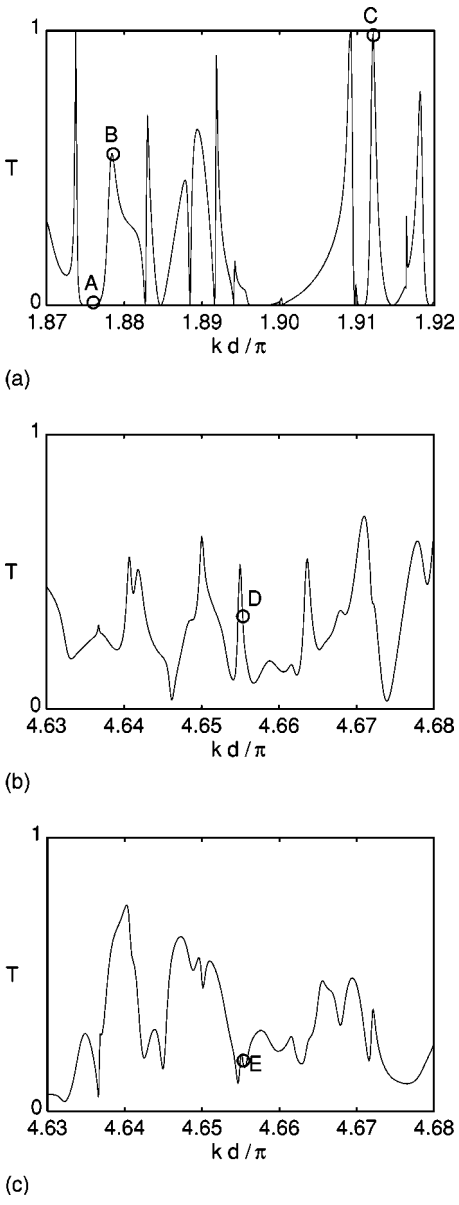

FIG. 1. Transmission probability as a function of Fermi wave number for the open stadium billiard. (a) A low-energy region for $n=1$. (b) A high-energy region for $n=1$. (c) A high-energy region for $n=4$.

as the coincidence of the nodal lines between Re ψ and Im ψ in Fig. 3(a).

In Fig. 3(b), we find a ''turbulence'' corresponding to the so-called bouncing-ball mode in the central region of the stadium cavity. We see 14 vertical nodes associated with marginally stable classical orbits bouncing vertically between the straight edges. Bouncing-ball states are nonstatistical states since the amplitude of ψ is strongly localized in the middle region of the stadium (the space reciprocity holds locally) and is very small in the endcaps (the space reciprocity does not necessarily hold). As a result, the head and tail of $P(|\psi|^2)$ for such states dominate [see Fig. 2(b)]. In order to evaluate the effect of the bouncing-ball structure itself on the wave statistical properties, we consider closed integrable rectangle billiards. The probability distribution and spatial

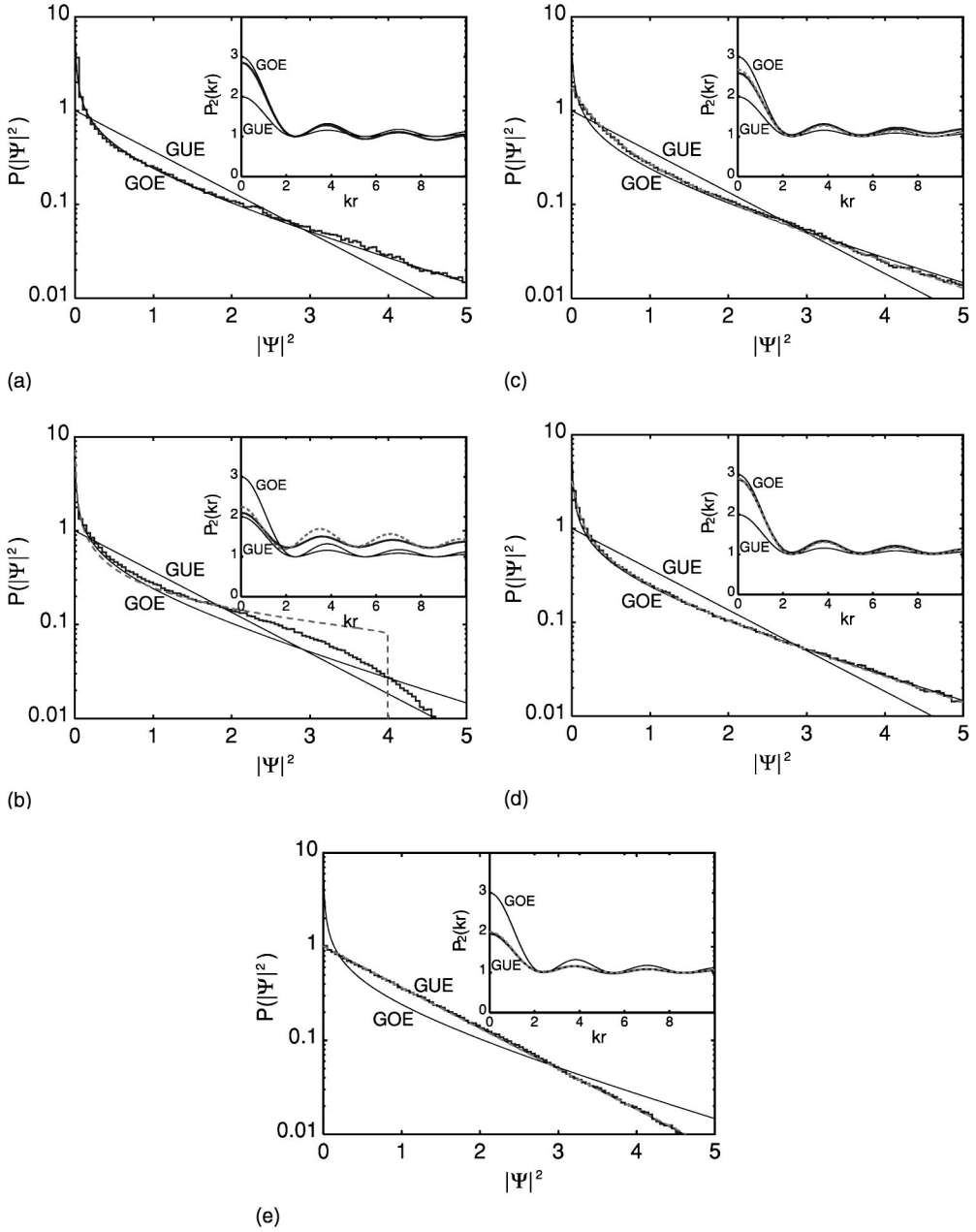

FIG. 2. Probability distribution (thick steps) and spatial correlation (thick line in the inset) of local densities in the open stadium billiard for the condition (a) *A*, (b) *B*, (c) *C*, (d) *D*, and (e) *E* in Fig. 1. Two thin lines show GOE and GUE cases (the same for the inset). Dashed thick line in (b) is Eq. (4.1) [Eq. (4.2) for the inset] for the eigenstate with a pair of quantum numbers (1,15) and $kd/\pi = 1.879\,16$ in the closed square billiard corresponding to the middle region of the stadium billiard. Dotted thick line in (c), (d) and (e) is Eq. (1.5) [Eq. (1.6) for the inset] for $b = 1.10$, 1.03 and 1.74, respectively.

correlation of the local wave densities in such systems show strong deviations from the GOE predictions [29]. The analytical form of the probability distribution is derived (see Appendix A) as

$$P(y) = \frac{1}{\pi^2 \sqrt{y}} K\left(\sqrt{1 - \frac{y}{4}} \right), \tag{4.1}$$

where $K(x)$ $(0 \leqslant x < 1)$ is the argument of the complete elliptic integral of the first kind with the amplitude $\pi/2$. The universal equation (4.1) is independent of quantum numbers and the aspect ratio of the rectangle. Correspondingly, the analytical form of the spatial correlation is also derived (see Appendix B) as

$$P_2(kr) = 1 + \frac{1}{2}[J_0(2kr\cos\gamma) + J_0(2kr\sin\gamma)] + \frac{1}{4} J_0(2kr), \tag{4.2}$$

where $\gamma = \tan^{-1}(k_1/k_2)$ (k_1 and k_2 are quantized wave num-

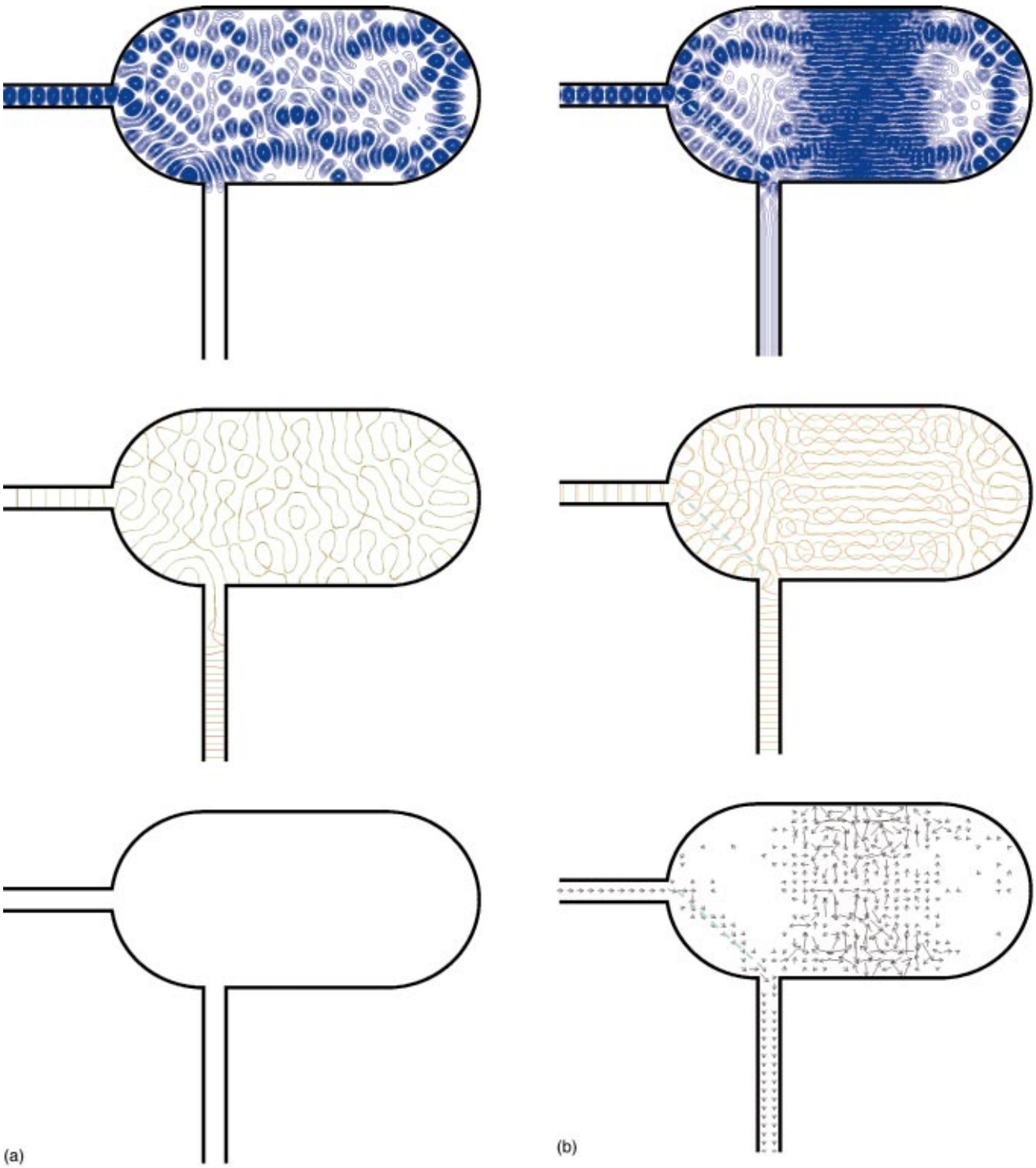

FIG. 3. (Color) Contour plot of wave probability density (top), nodal lines (middle; red lines for Re ψ and green lines for Im ψ), and probability current (bottom) in the open stadium billiard for the condition (a) *A*, (b) *B*, (c) *C*, (d) *D*, and (e) *E* in Fig. 1. Initial wave comes through the left lead into the cavity. The contours show about 97.5% of the largest wave probability density. Dotted light-blue lines in (b) and (d) show some of the short classical orbits corresponding to the localization of the wave probability density.

bers corresponding to two sides of the rectangle). We choose an eigenstate of a square billiard with a pair of quantum numbers (1,15) and $kd/\pi = 1.879\,16$ that are almost identical to the condition *B*, and Eqs. (4.1) and (4.2) are plotted in Fig. 2(b). We see that these analytical equations successfully describe the tendency of the overall deviations from the RMT predictions. More precise analytical agreements with the numerical results may be obtained by taking into account the

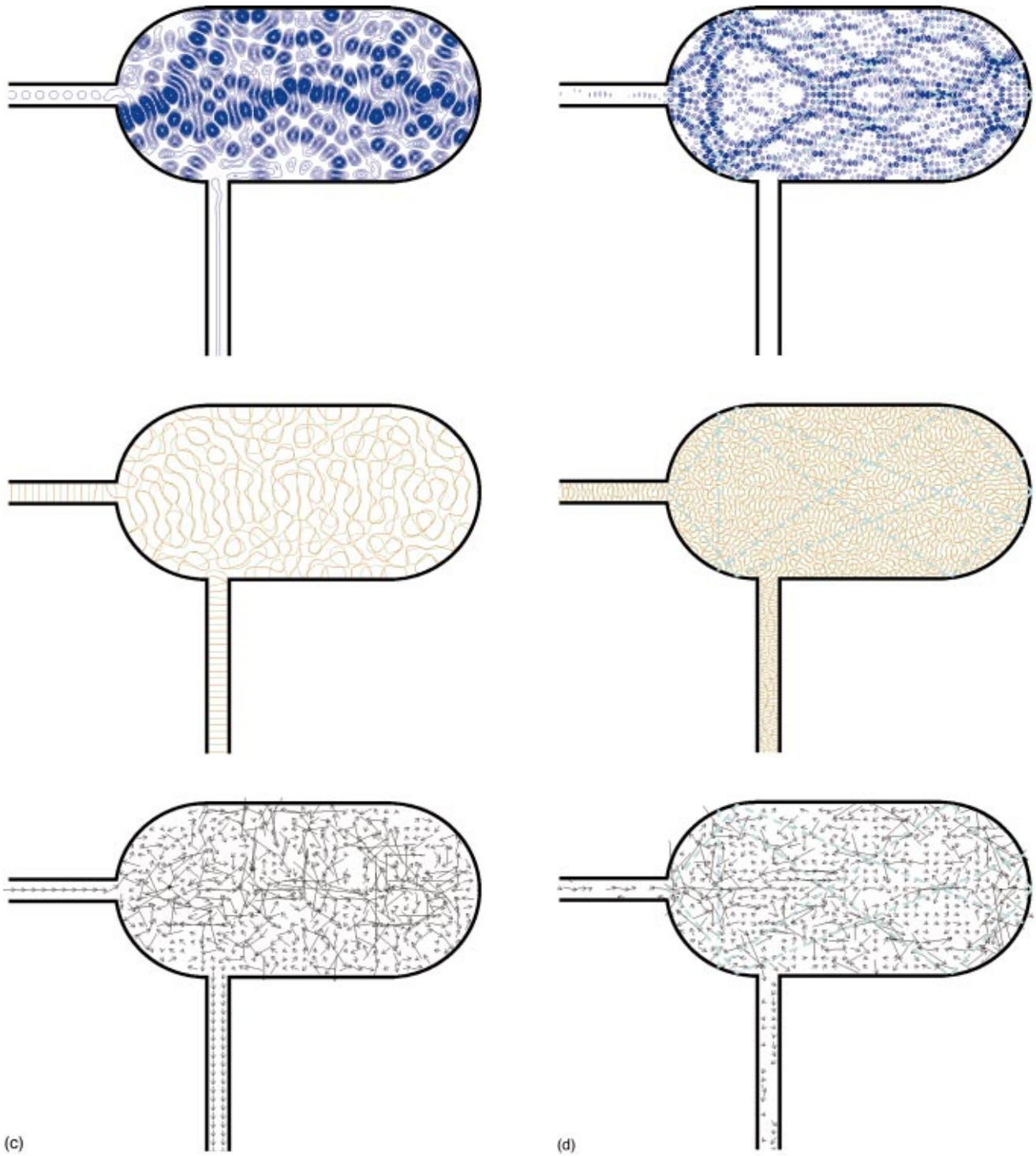

FIG. 3. (*Continued*).

coexistence of regular (bouncing-ball) and chaotic wave-function regions in the cavity (see Appendix C for a proposed analytical simple model).

In Fig. 3(c), we see fully chaotic probability-density structures in the cavity region with almost no reflection [see in the nodal pattern in the left lead that the phase difference between Re ψ and Im ψ is $\pi/2$, showing plane-wave propagation in one (right) direction]. In this case, we may expect the GUE statistics. However, the nodal lines between Re ψ and Im ψ are somewhat correlated as we see in Fig. 3(c), so that both $P(|\psi|^2)$ and $P_2(kr)$ show the intermediate between the GOE and GUE predictions [see Fig. 2(c)]. They are quantitatively consistent with Eqs. (1.5) and (1.6) with $b=1.10$ obtained numerically for ψ, which is close to the GOE case.

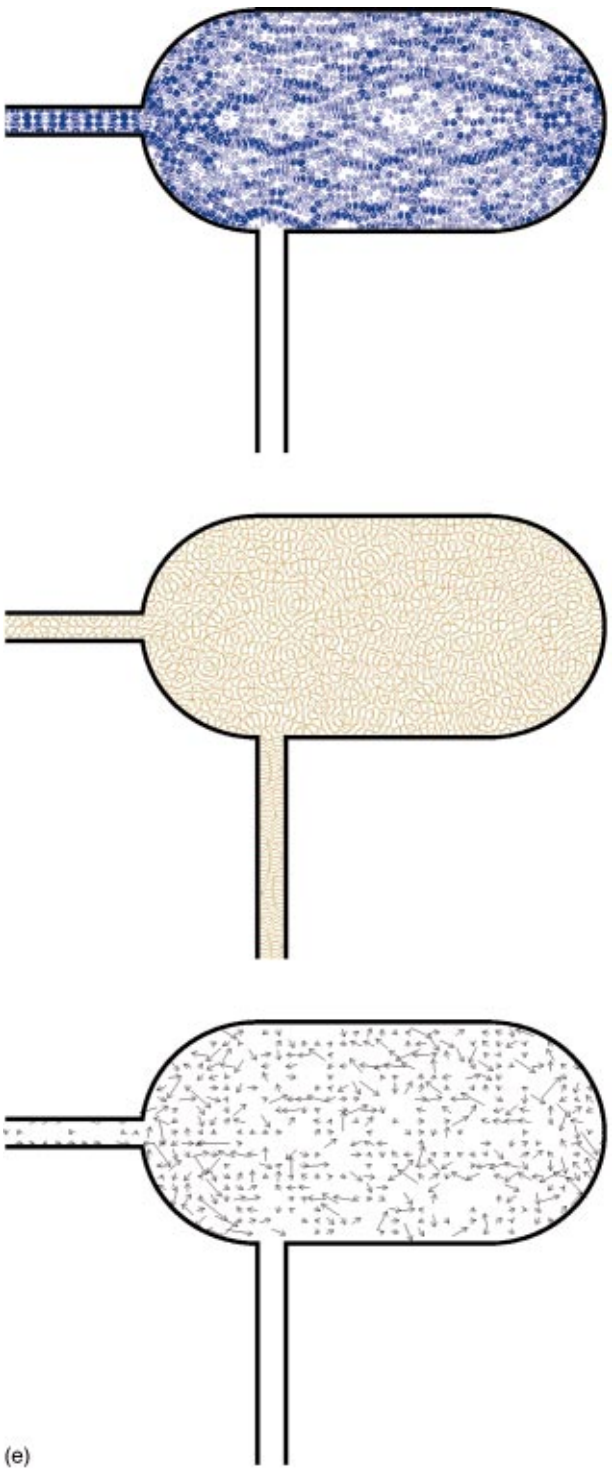

FIG. 3. (*Continued*).

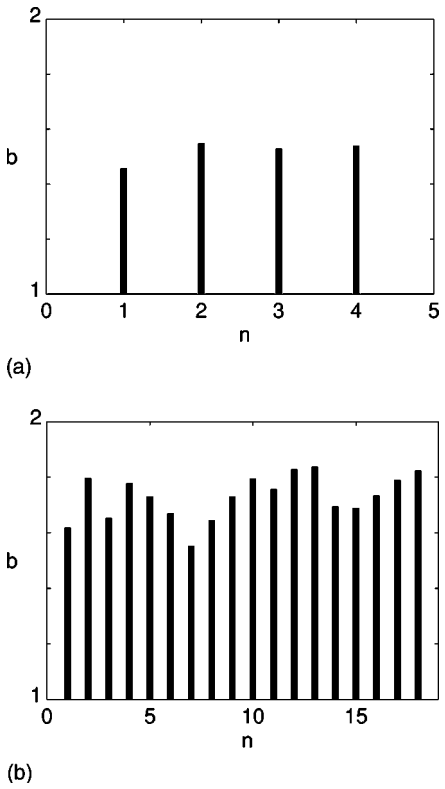

FIG. 4. Transition parameter vs initial mode for the open stadium billiard. (a) The case of leads shown in Fig. 3. The value of b was obtained as an average for $4.643\,35 \leqslant kd/\pi \leqslant 4.667\,22$. (b) The case of leads four times wider than those shown in Fig. 3. The value of b was obtained as an average for $18.573\,38 \leqslant kd/\pi \leqslant 18.668\,88$.

In general, the wave statistics show the GOE behaviors in the low-energy region ($N=1$, where N is the number of transmittable mode in the leads) as was first reported in Ref. [29]. The reason is that the difference of the boundary condition that Re ψ and Im ψ ''feel'' at the entrance of the cavity is relatively small in the low-energy case, so that Re ψ and Im ψ respond in almost the same manner, each of them producing similar nodal patterns. This is certified by the fact that b becomes large as d increases keeping the energy fixed (not shown here).

In the high-energy region ($N=4$), Fig. 2(e) shows that both $P(|\psi|^2)$ and $P_2(kr)$ are successfully described by Eqs. (1.5) and (1.6), respectively, with $b=1.74$ obtained numerically for ψ, which is very close to the GUE case. Figure 3(e) confirms the uncorrelated nodal lines between Re ψ and Im ψ in the cavity region. As we notice, the complete GUE statistics is conjectured to be obtained only in the high-energy (semiclassical) limit. Our investigations show that, until the energy reaches such a limit, the wave-function statistics demonstrate the crossover from the GOE to the GUE statistics by increasing the energy. Generic features of $P(|\psi|^2)$ and $P_2(kr)$ in this crossover regime can be described quantitatively by Eqs. (1.5) and (1.6), respectively, with increasing b, which is independent of the initial mode n for a fixed d (for numerical evidences, see Fig. 4). We should note that the statistics of Re ψ (or Im ψ) in general shows the GOE in spite of the crossover behavior of ψ (not shown here).

Another possibility of the departure from the GUE is a localization effect reminiscent of the phenomenon known as ''scar'' [30] describing an anomalous localization of quantum probability density along unstable periodic orbits in classically chaotic systems. The localization effect on wave-function intensity statistics has been examined using a time-dependent approach, i.e., in terms of recurrences of a test Gaussian wave packet, for closed and weakly (imperfectly)

open systems [31–33]. They showed that the tail of the wave-function intensity distribution in phase space is dominated by scarring, departing from the RMT predictions.

In contrast, the most prominent effect of the localization of wave probability density in perfectly open billiards is the local space reciprocity holding along the classical orbits corresponding to the localization not strongly coupled to any (open) transmission channel [see Fig. 3(d)]: Along such orbits, nodal lines of Re ψ and Im ψ coincide, indicating coherent overlap of time-reversed waves, and hence carrying no net current. As a result, both $P(|\psi|^2)$ and $P_2(kr)$ are close to the GOE predictions [see Fig. 2(d)], and surprisingly in excellent agreement with Eqs. (1.5) and (1.6), respectively, with $b=1.03$ obtained numerically for ψ.

In the case of ''localization'' strongly coupled to both the initial and one of the (open) transmission channels, the phase difference between Re ψ and Im ψ along the corresponding classical orbits is $\pi/2$, which indicates plane-wave propagation with nonzero probability current, resulting in anomaly of the wave statistics. The localization depicted with a dotted line in Fig. 3(b) is an example of this case, though the coupling to the transmission channel is not so strong, as we can infer from both the value of T and the amount of phase difference.

Finally, we note that, in the case of open integrable circle billiards, our numerical calculations show much peculiar behaviors of $P(|\psi|^2)$ and $P_2(kr)$ depending on the energy (not shown here). This fact suggests that neither $P(|\psi|^2)$ nor $P_2(kr)$ have universal expressions in the case of open integrable billiards.

V. CONCLUSIONS

In conclusions, our numerical analyses show that chaotic-scattering wave functions in open systems can be quantitatively interpreted in terms of statistically independent real and imaginary random fields. Statistical deviations from RMT are discussed in terms of the coexistence of regular and chaotic waves. This work leads to a deeper insight into the connection between the wave-function statistics in chaotic open systems and the RMT for the time-reversal symmetry-breaking crossover regime in closed systems. The properties of nodal structures in the wave dynamics have a close connection with the current statistics [12].

The results presented in this paper are also relevant for the Poynting vector describing the electromagnetic energy transport through a thin microwave resonator [34], as well as for sound propagation through an acoustic resonator [35,36]. We propose that experiments performed in such devices will yield statistical properties described with the formalism presented in this paper, and hence successfully verify theoretical predictions for a completely open ballistic system.

ACKNOWLEDGMENTS

One of the authors (H.I.) thanks B. S. Yamada for his numerical implementations and discussions at the early stage of this work. We also acknowledge support from the Swedish Board for Industrial and Technological Development (NUTEK) under Project No. P12144-1., the Swedish Royal Academy of Sciences, the Swedish Institute, INTAS Grant No. 97-11134, and the Russian Foundation for Basic Research (RFBR) Grant No. 00-02-16167. Part of the calculations were carried out by using a resource in the National Supercomputer Center (NSC) at Linköping.

APPENDIX A: PROBABILITY DISTRIBUTION OF EIGENFUNCTIONS IN RECTANGLE BILLIARDS

A standard eigenfunction of a rectangle billiard is

$$\psi(\mathbf{r})=A\sin(k_1x_1)\sin(k_2x_2), \tag{A1}$$

where $k_1^2+k_2^2=k^2$ and A is an arbitrary constant. From the statistical point of view where we make a space average over all the interior of the billiard, we can replace the arguments of the eigenfunction by $k_1x_1=\alpha$ and $k_2x_2=\beta$, where α and β are statistically independent random values uniformly distributed over an interval $[-\pi,\pi]$. Therefore, we can write the pseudorandom wave-density field, $\rho(\mathbf{r})\equiv|\psi(\mathbf{r})|^2$, in the form,

$$\rho=A^2\sin^2\alpha\sin^2\beta, \tag{A2}$$

and obtain the value of its average as

$$\langle\rho\rangle=A^2\langle\sin^2\alpha\rangle\langle\sin^2\beta\rangle=\frac{A^2}{4}. \tag{A3}$$

We normalize ψ in such a way that $\langle\rho\rangle=1$, i.e., $A=2$. We also obtain

$$\langle\rho^2\rangle=16\langle\sin^4\alpha\rangle\langle\sin^4\beta\rangle=9/4=2.25. \tag{A4}$$

The distribution function of the eigenfunction density (A2) is

$$g(\rho)=\langle\delta(\rho-pq)\rangle, \tag{A5}$$

where $p\equiv2\sin^2\alpha$ and $q\equiv2\sin^2\beta$ are statistically independent random variables with the identical distribution:

$$f(z)\equiv\langle\delta(z-p)\rangle=\langle\delta(z-q)\rangle=\frac{1}{\pi\sqrt{z(2-z)}}. \tag{A6}$$

Equation (A5) can be written as

$$g(\rho)=\int\int\delta(\rho-pq)f(p)f(q)dp\,dq=\int f(p)f\left(\frac{\rho}{p}\right)\frac{dp}{p}. \tag{A7}$$

Substituting the distribution (A6) into Eq. (A7), we get

$$g(\rho)=\frac{1}{\pi^2\sqrt{\rho}}\int_\rho^4\frac{dz}{\sqrt{z(4-z)(z-\rho)}} \tag{A8}$$

or equivalently

$$g(\rho)=\frac{1}{\pi^2\sqrt{\rho}}K\left(\sqrt{1-\frac{\rho}{4}}\right)\quad(0<\rho<4), \tag{A9}$$

where $K(z)$ $(0 \leqslant z < 1)$ is the argument of the complete elliptic integral of the first kind with the amplitude $\pi/2$. In two limits, $g(\rho \to 0) \sim [2/(\pi^2\sqrt{\rho})]\ln(1/\rho^2)$ and $g(4) = (4\pi)^{-1}$. The universal equation (A9) is independent of the quantization $\{k_1, k_2\}$ and the aspect ratio of the rectangle. Finally, we note that Eq. (A9) has a logarithmic correction for $\rho \to 0$ by comparison with the singularity $\sim 1/\sqrt{2\pi\rho}$ of the PT distribution (1.1). This logarithmic correction is stipulated by the presence of intersection points of nodal lines in integrable billiards. The absence of the logarithmic factor for the PT distribution is a witness of self-avoiding nature of nodal lines in the case of chaotic billiards [37].

APPENDIX B: SPATIAL CORRELATION OF EIGENFUNCTIONS IN RECTANGLE BILLIARDS

In the analysis of the spatial correlation, it is broadly accepted to carry out not only averaging over the space of the billiard but additional rotation of the vector **s** that prescribes the distance of two sampling points **r** and **r**+**s**. We write the components of the vector **s** as

$$s_1 = s\cos\theta, \quad s_2 = s\sin\theta, \tag{B1}$$

where $s \equiv |s|$ and θ is a random angle uniformly distributed over an interval $[-\pi, \pi]$. Then the correlation function of the normalized eigenfunction, $\psi(\mathbf{r}) = 2\sin(k_1 x_1)\sin(k_2 x_2)$, is equal to

$$a(s) = 4\langle \sin(\alpha)\sin(\alpha + k_1 s\cos\theta)\sin(\beta)\sin(\beta + k_2 s\sin\theta)\rangle, \tag{B2}$$

where $\alpha(\equiv k_1 x_1)$, $\beta(\equiv k_2 x_2)$, and θ are statistically independent random values uniformly distributed over $[-\pi, \pi]$. Carrying out averaging over α and β, we obtain

$$a(s) = \langle \cos(k_1 s\cos\theta)\cos(k_2 s\sin\theta)\rangle \tag{B3}$$

or, rewriting $k_1 \equiv k\cos\gamma$ and $k_2 \equiv k\sin\gamma$ $(k_1^2 + k_2^2 = k^2)$,

$$a(s) = \frac{1}{2}\langle [\cos(ks\cos(\gamma + \theta)) + \cos(ks\cos(\gamma - \theta))]\rangle. \tag{B4}$$

Here the angular brackets means averaging over the random θ. After carrying out this averaging, we obtain a Bessel correlation function,

$$a(s) = J_0(ks), \tag{B5}$$

which is similar to Eq. (1.3). Nevertheless, the correlation function of the local density, $\rho(\mathbf{r})$, significantly differs from Eq. (1.4), as is shown below.

The correlation function $b_\rho(s) = \langle \rho(\mathbf{r})\rho(\mathbf{r}+\mathbf{s})\rangle$ is reduced to the expression,

$$b_\rho(s) = 16\langle \sin^2(\alpha)\sin^2(\alpha + k_1 s\cos\theta)\sin^2(\beta) \times \sin^2(\beta + k_2 s\sin\theta)\rangle, \tag{B6}$$

or, after averaging over the statistically independent α and β,

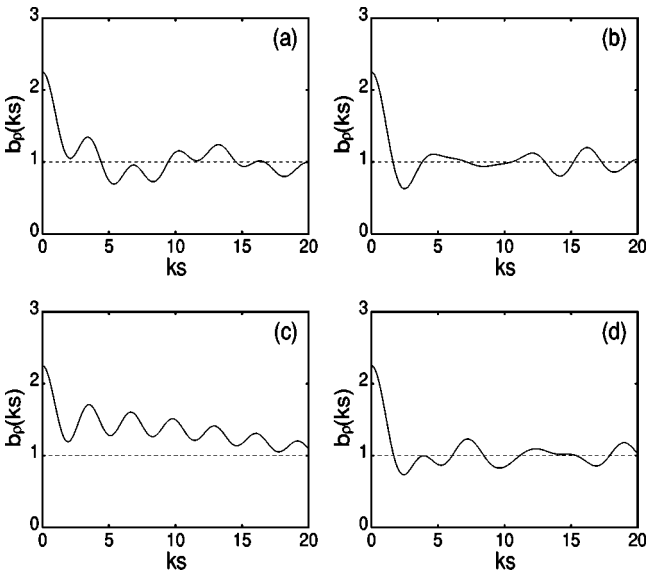

FIG. 5. Spatial correlation of local densities in the rectangle (square) billiard with Dirichlet conditions at the boundaries. Denoting two sides of the rectangle, a and b, and corresponding quantum numbers, m and n. We choose $k_1(=m\pi/a)$ and $k_2(=n\pi/b)$ as (a) $(a,b) = (25\pi, 25\pi)$. $(m,n) = (7.24)$: (b) $(a,b) - (25\pi, 25\pi)$, $(m,n) = (15,20)$; (c) $(a,b) = (2.485\,82, 2.872\,93)$; $(m,n) = (1.22)$: (d) $(a,b) = (2.485\,82, 2.872\,93)$, $(m,n) = (16,11)$.

$$b_\rho(s) = \frac{1}{4}\langle [2 + \cos(2k_1 s\cos\theta)][2 + \cos(2k_2 s\sin\theta)]\rangle, \tag{B7}$$

where the angular brackets means averaging over the random θ. After carrying out this averaging, we obtain the final form:

$$b_\rho(s) = 1 + \frac{1}{2}[J_0(2k_1 s) + J_0(2k_2 s)] + \frac{1}{4}J_0(2ks). \tag{B8}$$

Contrary to the probability distribution (A9), the correlation function of $\rho(\mathbf{r})$ does not have the same kind of universality for the quantization $\{k_1, k_2\}$ and the aspect ratio of the rectangle. We show some examples of $b_\rho(s)$ for different pairs of $\{k_1, k_2\}$ (see Fig. 5). There we find that the correlation function $b_\rho(s)$ significantly differs for different choices of k_1 and k_2 and converges as $b_\rho(0) = 9/4$ and $b_\rho(\infty) = 1$.

APPENDIX C: PROBABILITY DISTRIBUTION OF EIGENFUNCTIONS WITH MIXING CHAOTIC AND REGULAR STRUCTURES

We discussed that the PT distribution (1.1) applies to real chaotic eigenfunctions and Eq. (4.1) to eigenfunctions of rectangle billiards. In realistic situations in experimental measurements or numerical simulations, however, such a purely chaotic or regular state hardly arise. Instead we often see mixing of chaotic fields and some resonant regular modes. So it is worth proposing some simple model of wave-density distribution in the case of mixing chaotic and regular wave functions.

The simplest model for such a situation may be

$$\psi = \frac{u + \epsilon\varphi}{\sqrt{1+\epsilon^2}}. \tag{C1}$$

Here u is a Gaussian random variable with zero mean and unit variance, and describing a chaotic field. φ is a contribution of a regular eigenfunction of a rectangle billiard, and expressed as

$$\varphi = 2 \sin\alpha \sin\beta, \tag{C2}$$

where α and β are statistically independent values uniformly distributed over an interval $[-\pi,\pi]$. In Eq. (C1), a mixing parameter ϵ prescribes the degree of φ contribution to u and is essentially different from the GOE-GUE transition parameter ϵ (and b).

We recall a general probabilistic relation tying up together the distribution $f(x)$ of an arbitrary random value X and the distribution $g(z)$ of its square $Z=X^2$:

$$g(z) = \frac{1}{2\sqrt{z}}[f(\sqrt{z}) + f(\sqrt{-z})] \quad (z>0). \tag{C3}$$

From Eq. (4.1), the probability distribution of φ is found to be

$$P(\varphi) = \frac{1}{\pi^2} K\left(\sqrt{1-\frac{\varphi^2}{4}}\right) \quad (-2<\varphi<2). \tag{C4}$$

Therefore, the distribution of the entire mixed wave function (C1) is

$$f_\epsilon(\psi) = \frac{2}{\pi^2}\sqrt{\frac{1+\epsilon^2}{2\pi}} \int_{-1}^{1} \exp\left[-\frac{1}{2}(\psi\sqrt{1+\epsilon^2} - 2\epsilon\mu)^2\right] K(\sqrt{1-\mu^2})\, d\mu. \tag{C5}$$

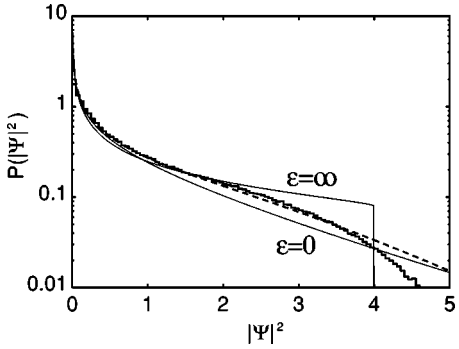

FIG. 6. Probability distribution of local densities of the mixed wave function (C1). Dotted thick line shows $g_\epsilon(\rho)$ for $\epsilon = 4/(\pi+4)(=\mathcal{S}/\mathcal{A})$. Two thin lines correspond to the cases of $\epsilon=0$ and $\epsilon=\infty$. Thick steps are the same as are depicted in Fig. 2(b).

Correspondingly, the distribution of the wave density, ρ $(=\psi^2)$, is described from Eq. (C3) by

$$g_\epsilon(\rho) = \frac{f_\epsilon(\sqrt{\rho})}{\sqrt{\rho}}. \tag{C6}$$

It becomes Eq. (1.1) in the case $\epsilon=0$ and Eq. (4.1) in the limit $\epsilon\to\infty$. In Fig. 6, $g_\epsilon(\rho)$ is plotted in comparison with our numerical data [the same shown in Fig. 2(b)] of the open stadium billiard. There it is assumed that the regular wave in the central area $\mathcal{S}$ lying between the straight segments of the stadium is overlapped with the chaotic wave developed in the entire area $\mathcal{A}$ of the cavity. Reflecting the fact that the data in Fig. 2(b) is in the case of low-energy region where the real and imaginary parts of the wave function are somewhat correlated with each other in the entire region of the cavity [see Fig. 3(b)], the model (C1) based on mixing of real chaotic and regular waves shows rather good agreement with our numerical data [except the long tail $\rho \gtrsim 3.6$, where the singularity of the distribution (C4) at $\rho=4$ plays a significant role] in spite of the simplification of the model.

[1] For a review, see T. Guhr, A. M.-Groeling, and H. A. Weidenmüller, Phys. Rep. **299**, 189 (1998).
[2] M. V. Berry and M. R. Dennis, Proc. R. Soc. London, Ser. A **456**, 2059 (2000).
[3] S. W. McDonald and A. N. Kaufman, Phys. Rev. Lett. **42**, 1189 (1979).
[4] C. Porter and R. Thomas, Phys. Rev. **104**, 483 (1956).
[5] V. N. Prigodin, Phys. Rev. Lett. **74**, 1566 (1995).
[6] M. V. Berry, J. Phys. A **10**, 2083 (1977).
[7] V. N. Prigodin, B. L. Altshuler, K. B. Efetov, and S. Iida, Phys. Rev. Lett. **72**, 546 (1994).
[8] K. Życzkowski and G. Lenz, Z. Phys. B: Condens. Matter **82**, 299 (1991).
[9] G. Lenz and K. Życzkowski, J. Phys. A **25**, 5539 (1992).
[10] E. Kanzieper and V. Freilikher, Phys. Rev. B **54**, 8737 (1996).
[11] R. Pnini and B. Shapiro, Phys. Rev. E **54**, R1032 (1996).
[12] A. I. Saichev, H. Ishio, A. F. Sadreev, and K.-F. Berggren (unpublished).
[13] S.-H. Chung, A. Gokirmak, D.-H. Wu, J. S. A. Bridgewater, E. Ott, T. M. Antonsen, and S. M. Anlage, Phys. Rev. Lett. **85**, 2482 (2000).
[14] J. Brickmann, Y. M. Engel, and R. D. Levine, Chem. Phys. Lett. **137**, 441 (1987).
[15] H.-J. Sommers and S. Iida, Phys. Rev. E **49**, R2513 (1994).
[16] V. I. Fal'ko and K. B. Efetov, Phys. Rev. B **50**, 11 267 (1994).
[17] A. Kudrolli, V. Kidambi, and S. Sridhar, Phys. Rev. Lett. **75**, 822 (1995).
[18] D. H. Wu, J. S. A. Bridgewater, A. Gokirmak, and S. M. Anlage, Phys. Rev. Lett. **81**, 2890 (1998).
[19] M. Shapiro and G. Goelman, Phys. Rev. Lett. **53**, 1714 (1984).
[20] S. W. McDonald and A. N. Kaufman, Phys. Rev. A **37**, 3067 (1988).
[21] R. Aurich and F. Steiner, Physica D **64**, 185 (1993).
[22] B. Li and M. Robnik, J. Phys. A **27**, 5509 (1994).
[23] B. Li and B. Hu, J. Phys. A **31**, 483 (1998).
[24] P. Šeba, F. Haake, M. Kuś, M. Barth, U. Kuhl, and H.-J.

Stöckmann, Phys. Rev. E **56**, 2680 (1997).
[25] L. A. Bunimovich, Funct. Anal. Appl. **8**, 254 (1974).
[26] G. Benettin and J. M. Strelcyn, Phys. Rev. A **17**, 773 (1978).
[27] K. Nakamura and H. Ishio, J. Phys. Soc. Jpn. **61**, 3939 (1992).
[28] R. Landauer, IBM J. Res. Dev. **1**, 223 (1957).
[29] K. Yamada, B. S. thesis, Osaka Kyoiku University, 1998.
[30] E. J. Heller, Phys. Rev. Lett. **53**, 1515 (1984).
[31] L. Kaplan, Nonlinearity **12**, R1 (1999).
[32] L. Kaplan, Phys. Rev. Lett. **80**, 2582 (1998).
[33] L. Kaplan and E. J. Heller, Ann. Phys. (N.Y.) **264**, 171 (1998).
[34] H.-J. Stöckmann, *Quantum Chaos: An Introduction* (Cambridge University Press, Cambridge, UK, 1999).
[35] K. Schaadt, M.S. thesis, Niels Bohr Institute, Copenhagen. 1997, http://www.nbi.dk/~schaadt/speciale/speciale.ps.gz
[36] C. Ellegaard, K. Schaadt, and P. Bertelsen, in Proceedings of the Nobel Symposium on Quantum Chaos. 2000, edited by K.-F. Berggren and S. Eberg [Phys. Scr. **T90**, 60 (2001)].
[37] A. I. Saichev, K. F.-Berggren, and A. F. Sadreev, Phys. Rev. E **64**, 036222 (2001).